Electronic Structure of Intentionally Disordered AlAs/GaAs Superlattices

Kurt A. Mäder, Lin-Wang Wang, and Alex Zunger

National Renewable Energy Laboratory, Golden, Colorado 80401
(Received 5 October 1994)

We use realistic pseudopotentials and a plane-wave basis to study the electronic structure of nonperiodic, three-dimensional, 2000-atom $(AlAs)_n/(GaAs)_m$ (001) superlattices, where the individual layer thicknesses $n, m \in \{1, 2, 3\}$ are randomly selected. We find that while the band gap of the equivalent ($n = m = 2$) *ordered* superlattice is indirect, random fluctuations in layer thicknesses lead to a *direct* gap in the planar Brillouin zone, strong wave function localization along the growth direction, short radiative lifetimes, and a significant band-gap reduction, in agreement with experiments on such intentionally grown disordered superlattices.

Ordered semiconductor superlattices—produced routinely by epitaxial crystal growth techniques—are widely recognized for their unique electronic and optical properties [1]. To tailor the electronic properties (e.g., through band folding) one aims at growing ordered superlattices (o-SL) with *definite values* of the thicknesses n and m in $(A)_n/(G)_m$. One could, however, deliberately grow a *disordered* superlattice (d-SL) [2,3], where the individual layer thicknesses $n, m, n', m', n'', m'', \ldots$ are selected at random according to a given probability distribution $p_\alpha(n)$ ($\alpha = A, G$). While the electronic structure of an o-SL is characterized by extended states and the formation of minibands, a truly one-dimensional disordered system (described, e.g., by the Anderson model) shows carrier localization and absence of dispersion [4,5]. Sasaki *et al.* [3] grew ~ 1000 monolayer (ML) thick AlAs/GaAs d-SL's (i.e., $A = $ AlAs, $G = $ GaAs) with n and m chosen from a set of small integers $\{1, 2, 3\}$, viz., $p_A = p_G = p$, with $p(1) = p(2) = p(3) = \frac{1}{3}$. Since the average layer thickness is 2 ML, one can think of this d-SL as evolving from an $(A)_2/(G)_2$ o-SL by random substitution of A_2 and G_2 layers by A_1, A_3, G_1, and G_3 layers ("δ doping"). Such disordered superlattices have shown surprising and unique optical properties relative to their parent o-SL [3]: (a) strong and initially fast decaying (lifetime $\tau = 0.25$ ns at $T = 77$ K) photoluminescence (PL) intensity even though the equivalent o-SL has an indirect band gap and thus emits both weakly and slowly, (b) a large redshift (~ 60 meV) of the PL peak with respect to the equivalent o-SL, and (c) an order of magnitude slower rate of reduction of the PL intensity with temperature. These unusual properties of d-SL's appear very attractive for optoelectronic applications [3].

In modeling the electronic structure of a d-SL [2,6,7], one faces difficulties arising from the existence of two entirely different length scales: (i) The lack of translational symmetry requires the use of unit cells with a macroscopic length $N \approx 1000$ ML, equal to the *total length* of the d-SL ($Nd \approx 300$ nm, where d is the monolayer thickness). (ii) The spatial variations of the electron potential,

however, occur on a microscopic length scale of about 0.1 nm. While it is possible to rescale the microscopic length scale by replacing the periodic atomic potential by an external, rectangular potential [2,6], this approach fails to describe the band structure [e.g., the indirect gap of the $(AlAs)_2/(GaAs)_2$ o-SL] in the present regime of rapid layer fluctuations. To overcome the problems arising from the existence of two disparate length scales, we extended a microscopic pseudopotential description of the electron structure to a macroscopic length scale necessitated by the absence of translational symmetry. We use *fixed* (screened) atomic pseudopotentials that were carefully fitted to bulk band structures, effective masses, deformation potentials, band offsets, and energy levels in superlattices [8]. The wave functions are expanded in about 30 plane waves per atom. For an N-monolayer superlattice along (001) with two atoms per monolayer the corresponding matrix dimension is therefore about $60N \times 60N$. Standard techniques to solve the Schrödinger equation require orthogonalization of the states of interest (i.e., near the band gap) to all lower-lying states. This leads to an N^3 scaling of the effort and becomes impractical for structures with $N \approx 100$ ML. We use instead the "folded-spectrum" method [9], where eigenstates are obtained directly in an energy window of interest (e.g., near the band gap), without having to solve for any of the $\sim 8N$ lower-lying eigenstates first, thus circumventing the need for orthogonalization. The effort scales linearly with N, allowing us to use the realistic, three-dimensional pseudopotentials, and to solve the Schrödinger equation in a highly flexible plane-wave basis even for $N = 1000$ ML.

Application to d-SL's of AlAs/GaAs leads to an explanation of the large redshift, the enhanced oscillator strength, and the weak temperature dependence in terms of band-edge wave-function localization. The source of localization is interesting: In truly one-dimensional disordered chains *all* states are, in general, localized [4,5]. However, the laboratory-grown [3] d-SL's have extended layers in the (x, y) plane (perpendicular to the disorder direction $z = [001]$), so these *quasi*-one-

dimensional systems retain, in fact, a three-dimensional character, and the states need not be localized by disorder. We will show that the localization in the d-SL originates mostly from the formation of impuritylike, localized bound states due to insertion of δ layers into the o-SL.

In Fig. 1(a) we show the planar wave function average $|\bar{\psi}_E(z)|^2 = \int d^2 r_\perp |\psi_E(r)|^2$ of a few occupied and unoccupied band-edge states of a d-SL with a 1000-monolayer unit cell. We see that these band-edge wave functions are sharply localized. We can quantify the effective localization length (in monolayer units) for the wave function ψ_E at energy E as [5]

$$L_{\text{eff}}(E) = \frac{1}{h}\left(\sum_i |\langle i|\bar{\psi}_E\rangle|^4\right)^{-1}, \qquad (1)$$

where the sum extends over the grid points i along z, and h is the number of grid points per monolayer. For a truly extended state, L_{eff} is of the order of N, while for a state localized on one site, $L_{\text{eff}} = 1$. We find that $L_{\text{eff}} \lesssim 15$ ML for the band-edge states. The asymptotic decay length γ^{-1} can be quantified by $\langle |\bar{\psi}_E(z)|\rangle \propto e^{-\gamma z}$, where the angular brackets denote averaging over the fast oscillations of $|\bar{\psi}_E(z)|$ along z. Near the band edges, the calculated values are $\gamma \approx 0.2$ ML^{-1}.

We now investigate two possible mechanisms for the wave function localization apparent in Fig. 1(a):
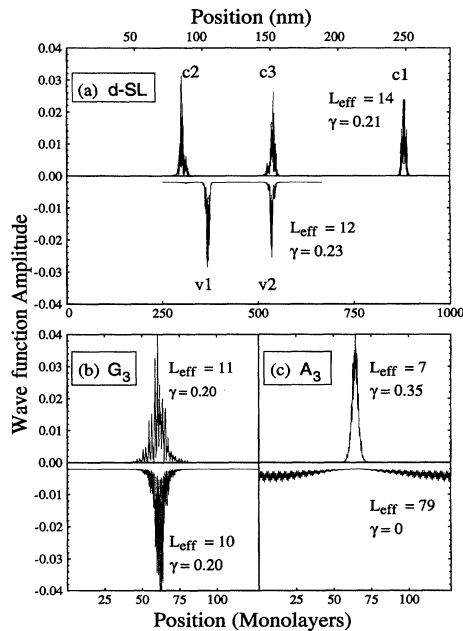

FIG. 1. Planar average of the wave functions squared in (a) a 1000-monolayer d-SL, (b) an o-SL host containing a single $(GaAs)_3$ δ impurity, and (c) a single $(AlAs)_3$ δ impurity. Unoccupied states are labeled $c1, c2, \ldots$; occupied states are labeled $v1, v2, \ldots$, and are plotted in the negative direction with a small offset for clarity. L_{eff} and γ are given in ML and ML^{-1}, respectively.

(i) chemical binding to δ-like "impurity layers" in an otherwise ordered $(A)_2/(G)_2$ host, and (ii) a continuous increase of localization (measured by γ or by L_{eff}^{-1}) with an increasing degree of disorder. Scenario (i) is motivated by the fact that in one dimension an attractive δ potential always has one bound state, whereas scenario (ii) is valid for the Anderson model with on-site disorder obeying a continuous probability distribution [5]. In our case of a discrete probability distribution $p(n)$, we connect the two pictures by starting with the reference o-SL $(A)_2/(G)_2$, and gradually substituting A_2 and G_2 layers by "wrong" layers with $n = 1$ or $n = 3$. We measure the degree of disorder by counting the relative frequency R of these layers, i.e.,

$$R = p(1)/p(2) = p(3)/p(2).$$

The fully disordered SL has $R = 1$, the single δ layer in an ordered $(A)_2/(G)_2$ superlattice corresponds to $R \approx N^{-1}$, while the perfect o-SL has $R = 0$.

To understand the possibility of impuritylike localization, consider, for example, a G_3 δ layer embedded in the otherwise perfect o-SL $\cdots A_2 G_2 A_2 G_2 A_2 G_2 \cdots$, thus converting it into $\cdots A_2 G_2 A_2 G_3 A_2 G_2 \cdots$. If the G_3 δ layer is attractive to electrons (holes), it will bind a state below the conduction-band minimum (CBM) [above the valence-band maximum (VBM)] of the o-SL [10]. We find that a $(GaAs)_3$ δ layer in the $(AlAs)_2/(GaAs)_2$ o-SL indeed binds an electron *and* a hole [Fig. 1(b)], while an $(AlAs)_3$ layer binds an electron but does not bind a hole [Fig. 1(c)]. The bound-state localization lengths γ^{-1} and L_{eff} obtained with a *single* δ layer are similar to those obtained in the fully disordered SL (Fig. 1), suggesting that the same mechanism of localization could be at work in both cases. As one increases the concentration R of randomly positioned δ layers, one finds more bound states which are eventually forming a quasicontinuum inside the band gap [11]. This is illustrated in Fig. 2, where the band-edge energies of d-SL's with $N = 128$ ML [12] are plotted as a function of the degree of disorder R. As R approaches zero, the band edges merge with the finite binding energies of an isolated δ layer [scenario (i)], and not with the unperturbed band edges of the o-SL [scenario (ii)]. This significant observation suggests that the localization energy in the d-SL comes mostly from impurity binding. Figure 2 shows that for large degrees of disorder R, the band edges are pushed further into the gap. To isolate the effect of pure disorder from the effect of impuritylike localization, we also show in Fig. 2 the band edges of an o-SL containing a *periodic array* of δ layers of concentration R, i.e., separated by a distance $\sim R^{-1}$. We see that even for an array of closely spaced δ layers ($R \rightarrow 1$), the binding energy does not increase, indicating a negligible interaction between the neighboring, *coherently arranged* bound states. In contrast, in a d-SL the δ-layer-like bound states are arranged *incoherently*, leading to a band tail. These studies show that the localization
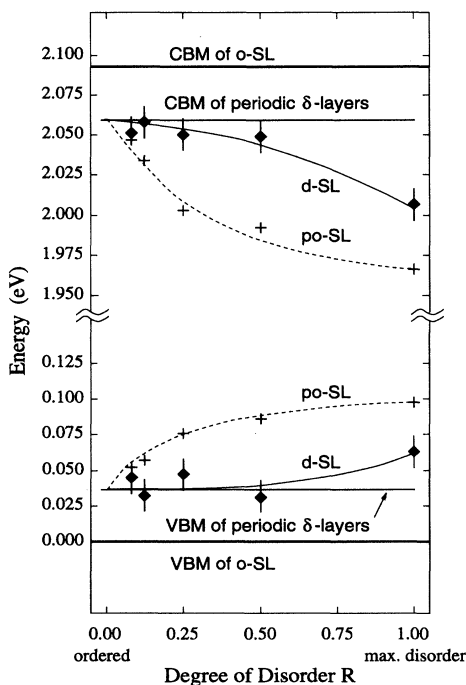
FIG. 2. Band-edge energies of disordered (d-SL, diamonds), partially ordered superlattices (po-SL, pluses), and a periodic array of δ layers embedded in an o-SL (thin horizontal lines) as a function of R [Eq. (2)]. Lines are guides to the eye. The thick horizontal lines denote the unperturbed band edges of the parent o-SL. The vertical bars on the d-SL data points denote the range of binding energies obtained from ~ 10 different realizations of a d-SL with length $N = 128$.

length of the band-edge states in a d-SL is decided already by the chemical, impuritylike binding of a single δ layer [Figs. 1(b) and 1(c)]. Furthermore, the energy position of the gap levels at small to intermediate degrees of disorder R is also determined by the properties of noninteracting, *periodically arranged* δ layers (Fig. 2). For higher values of R, disorder shifts and broadens the gap levels further into the gap, without modifying their localization length.

To illustrate the dependence of the gap-level shifts on the particular form of disorder, we compare the results obtained for the d-SL with those found in a partially ordered superlattice (po-SL): Arent *et al.* [13] grew po-SL's with the same distribution function $p(n)$ for the A_n layers as in a d-SL, but preserved long-range order by requiring that each A_n layer be followed by a G_{4-n} layer. Therefore, at positions $1, 5, 9, \ldots$ there is always an A layer, and at positions $4, 8, 12, \ldots$ there is always a G layer, while at the "sandwiched" positions, A and G layers are distributed randomly. We see in Fig. 2 that the presence of long-range order leads to an even larger shift of gap levels than in the equivalent d-SL at the same R value. The band-edge wave functions have the same characteristic L_{eff} and γ as in a d-SL. Thus, absence

of long-range order (in the d-SL) is not essential for obtaining large band-edge shifts.

The calculated band-gap reduction of the d-SL and po-SL with respect to the o-SL (Fig. 2) is consistent with experiment [3,13]: We find band gaps of 2.09, 1.94, and 1.87 eV for the o-SL, d-SL, and po-SL, respectively, compared with the experimental PL emission lines at 2.02, 1.96 [3], and 1.87 eV [13], respectively.

To determine if the d-SL has a direct or indirect gap in the two-dimensional Brillouin zone, we show in Fig. 3 the dispersion of the band-edge states of the d-SL (solid lines), o-SL (thin lines), and single δ layer (dotted lines) along the symmetry lines $\bar{\Sigma}$ and $\bar{\Delta}$, i.e., from $\bar{\Gamma}$ to $\bar{M} = \frac{1}{\sqrt{2}}(1,1)$ and from $\bar{\Gamma}$ to $\bar{X} = \frac{1}{\sqrt{2}}(1,0)$, respectively. The thin horizontal lines denote the band edges of the underlying o-SL. We find that the conduction bands of the d-SL dip below these lines. The difference ("binding energy") increases in the order $\bar{M} \rightarrow \bar{\Gamma} \rightarrow \bar{X}$ [14]. Thus, the large binding energy at $\bar{\Gamma}$ pulls the conduction-band edge below the one at $\bar{M}$ by 60 meV, *making the d-SL a direct-gap material* [15], even though the o-SL is indirect (with CBM at $\bar{M}$). This suggests strongly that the observed [3] strong PL intensity is due to the occurrence of a direct band gap, leading to efficient recombination of electrons and holes localized in the same spatial region along z [see, e.g., the same positions along the chain of
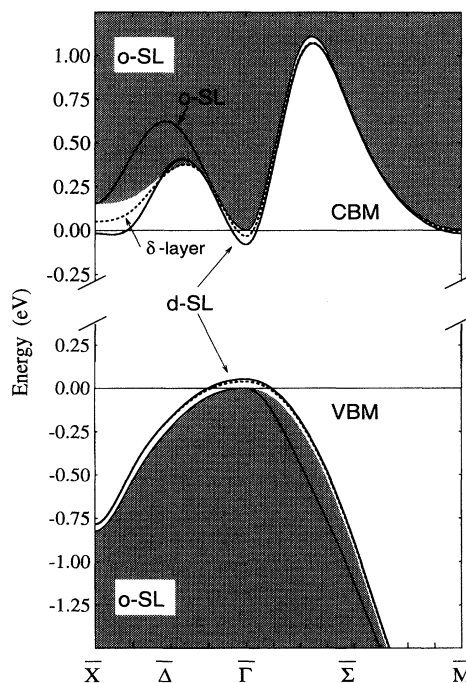

FIG. 3. Dispersion of the band-edge state in a d-SL (solid lines), o-SL (thin lines), and a single δ layer in an o-SL host (dotted lines) along the $\bar{\Delta}$ and $\bar{\Sigma}$ symmetry lines in the planar Brillouin zone. Also shown are the (001)-projected bands of the o-SL (shaded area). The supercell size was $N = 128$.

states $v2$ and $c3$ in Fig. 1(a)]. The localization along z relaxes the $k_\parallel$-selection rule, thus further enhancing the oscillator strength. The enhanced oscillator strength is reflected by short radiative lifetimes τ: we calculate $\tau = 1$ ns for the $v2 \to c3$ transition at energy 1.96 eV [Fig. 1(a)]. These radiative lifetimes are $1000\times$ faster compared to those measured in indirect-gap o-SL's ($\tau \approx 5.5~\mu$s at $T = 2$ K) [16].

To understand why the PL intensity in a d-SL has a weaker temperature dependence than in an o-SL, consider vertical transport to nonradiative recombination centers. This channel will be inhibited, unless there are strongly overlapping electron states within an energy $\sim kT$ of each other. Strong overlap occurs when $\zeta(E, T) = kT\rho(E_T)L_{\rm eff}(E_T) > 1$, where $\rho(E)$ is the one-dimensional density of states, and E_T is a typical energy that is thermally occupied at temperature T. Figure 4 shows $\rho(E)$, $L_{\rm eff}(E)$, and $\zeta(E, T)$ obtained by averaging over 100 realizations of $N = 2000$ ML d-SL's, calculated within the Kronig-Penney approximation with band offset fitted to our pseudopotential calculations. We find that (i) the DOS exhibits a ~ 200 meV wide band tail extending below the CBM of the o-SL (the zero of energy), (ii) $L_{\rm eff}$ is almost constant (~ 20 ML) in the band tail, and (iii) at the thermally populated levels [denoted by the arrows in Fig. 4(b)] $\zeta \ll 1$, thus vertical hopping is suppressed. Consequently, the d-SL will have a weaker temperature dependence of the PL decay, because higher temperatures

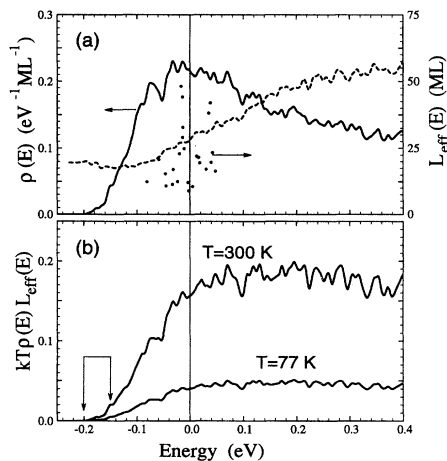will be needed to dissociate the electron-hole pairs in the vertical dimension.

FIG. 4. (a) Density of states $\rho(E)$ (solid line) and $L_{\rm eff}(E)$ (dashed line) averaged over 100 realizations of $N = 2000$ ML d-SL's, calculated with the Kronig-Penney model. Dots indicate $L_{\rm eff}(E)$ obtained for an $N = 128$ ML pseudopotential calculation. (b) The product $\zeta(E, T) = kT\rho(E)L_{\rm eff}(E)$.

[1] *Condensed Systems of Low Dimensionality,* edited by J. L. Beeby *et al.,* NATO ASI Ser. B, Vol. 253 (Plenum Press, New York, 1991).
[2] A. Chomette *et al.,* Phys. Rev. Lett. **57**, 1464 (1986).
[3] A. Sasaki *et al.,* Jpn. J. Appl. Phys. **28**, L1249 (1989); J. Cryst. Growth **115**, 490 (1991).
[4] R. E. Borland, Proc. R. Soc. London A **274**, 529 (1963).
[5] C. Papatriantafillou and E. N. Economou, Phys. Rev. B **13**, 920 (1976).
[6] L. Pavesi *et al.,* Phys. Rev. B **39**, 7788 (1989).
[7] E. G. Wang *et al.,* Appl. Phys. Lett. **64**, 443 (1994).
[8] K. A. Mäder and A. Zunger, Phys. Rev. B **50**, 17 393 (1994).
[9] L.-W. Wang and A. Zunger, J. Chem. Phys. **100**, 2394 (1994).
[10] K. A. Mäder and A. Baldereschi, Mater. Res. Soc. Symp. Proc. **240**, 597 (1992).
[11] I. M. Lifshits, Sov. Phys. JETP **17**, 1159 (1963); L. A. Pastur, *Introduction to the Theory of Disordered Systems* (Wiley and Sons, New York, 1987), p. 62.
[12] Note that in order to correctly describe localized wave functions we need $N \gg L_{\rm eff}$. We have confirmed that band-edge wave functions calculated in an $N = 128$ d-SL agree very well with those shown in Fig. 1(a), which were calculated with $N = 1000$.
[13] D. J. Arent *et al.,* Phys. Rev. B **49**, 11 173 (1994).
[14] The large binding energy at $\bar{X}$ is a consequence of the level repulsion of the folded L_{1c} states, which is much stronger for odd values of the repeat period n than for even n [see, for example, S.-H. Wei and A. Zunger, Appl. Phys. Lett. **53**, 2077 (1988)]. In the d-SL the odd-even selection rule is broken, leading to a stronger level repulsion in the d-SL than in the $n = 2$ o-SL.
[15] In a recent tight-binding study of an $N = 10$–20 ML model of a d-SL, Wang *et al.* [7] found a nearly dispersionless conduction band along $\bar{\Delta}$ and $\bar{\Sigma}$, an *indirect gap* at $\bar{M}$, and a 2–4 ML localization length. The differences with respect to the present pseudopotential calculation may reflect a combination of the use of rather short SL's and the restricted variational flexibility of the tight-binding method used in Ref. [7].
[16] W. Ge *et al.,* J. Lumin. **59**, 163 (1994).